

An Adaptive Fuzzy-Genetic Algorithm for estimating matrix physicochemical properties to achieve desired drug release profiles.

Geison P. Voga

*Departamento de Química-ICEx, Universidade Federal de Minas Gerais,
Pampulha (31.270-901) Belo Horizonte, MG-Brazil*

Domingos D. C. Rodrigues

*Centro Nacional de Processamento de Alto Desempenho,
Laboratório de Computação Científica-ICEx,
Universidade Federal de Minas Gerais,
Pampulha (31.270-901) Belo Horizonte, MG-Brazil*

Jadson C. Belchior*

*Departamento de Química-ICEx, Universidade Federal de Minas Gerais,
Pampulha (31.270-901) Belo Horizonte, MG-Brazil*

(Dated: February 19, 2009)

Abstract

*Electronic address: jadson@ufmg.br

I. INTRODUCTION

Over recent years there has been a growing interest in drug delivery studies from solid pharmaceutical dosage forms. Drug delivery systems (DDS hereinafter) must be developed taking into account the economical aspects involved in the industrial mass production, that is to say that DDS must be manufactured at low cost without compromising the therapeutic goal of the drug. This has prompted the pharmaceutical industry to search for new cheap raw materials for the manufacture of delivery systems and for the formulation of new encapsulation techniques ([13] and references therein). It is therefore important to be able to quantify the dependence of the transport mechanisms involved in the release of any drug from the physicochemical properties of the carrier material. In general the therapeutic treatments consist in delivering the drug to some specific region or organ of the body which therefore requires that the medication must be released in a controlled and sustained form to keep its concentration in the body at accepted levels. Due to ease of production and low cost associated, the usual procedure is to disperse some drug in a hydrophobic (e.g. or hydrophilic (e.g. hydroxypropyl methylcellulose-HPMC) biomaterial so that a controlled release of the drug into the biological medium can be attained. In the pharmaceutical literature this combination of drug and excipient agent is commonly referred as matrix. Overall the release of any drug from some matrix (consisting of bioceramics or biodegradable polymers) involves both the physical phenomena of dissolution or erosion and diffusion. Once the tablet carrying the drug in suspension enters in contact with water or the physiological fluid, the latter diffuses into the tablet (imbibition) increasing its volume (swelling) and promoting the drug dissolution. The dissolved drug will then diffuse out of the device due to steep concentration gradients. For water insoluble polymers, the diffusional mass transfer is preceded by cleavage of the polymer chains that constitute the matrix (erosion).

Several phenomenological models have been proposed with various degrees of sophistication to describe such processes in simple and compact mathematical forms (for a comprehensive review see [2]), but full treatment of the involved transport mechanisms often need to be done numerically. When no matrix erosion or swelling occurs (or they are instantaneous) and drug molecules do not interact, the release is basically controlled by the mechanism of Fickian diffusion which is a well understood process with a very precise mathematical formulation for any geometry of the device and deeply rooted in physical first principles ([3]).

Even so, simple analytical solutions are only obtained when one imposes strict assumptions, as constant drug diffusivity, perfect sink conditions, fixed boundaries and an infinite external medium. When dissolution or erosion becomes relevant, the resulting mathematical equations can get somewhat cumbersome as the drug diffusion in a substrate can depend on various parameters, such as the matrix composition, matrix geometry, volume expansion (swelling), erosion, polymer dissolution, initial drug loading and drug saturation solubility in the matrix [13, 15]. Therefore depending on the degree of simplification of the kinetics behind drug release, one can get an explicit or implicit analytical relation between the independent (mass-fraction of drug release and time) and dependent (physicochemical properties of the matrix) variables of the problem.

From the technological point of view, explicit analytical formulae as simple as possible are mostly desired in order to simulate and access the economical viability of alternative paths of the manufacturing of DDS in a rapid and efficient manner, as well as for routine quality control processes. Several statistical methods have been proposed to test the similarity between dissolution profiles of test and reference batches as well as to decide the best model to study the drug dissolution (we refer the reader to the review of Costa and Sousa Lobo [2]). Given the elevated number of variables involved, one does in practice several cuts in the parameter space and performs a nonlinear regression analysis to fit the experimental data to some chosen model [5]. Quite recently a complementary approach to these conventional methods based on artificial neural networks (ANN) has been used (see review of Sun *et al.* [17] and references therein). This approach has proved to be useful in predicting ideal experimental parameters for providing a controlled drug release. It uses the whole experimental data training set and correlates it with the input parameters of the chosen formulation by optimizing the weights and biases of the ANN through some minimization technique. There is no need to have *a priori* functional relationship between the dependent and independent variables although in practice one uses some accepted model to simulate a great number of experiments to increase the training set. After the training stage, one can quickly predict new formulation input parameters (geometry and physicochemical properties of the matrix) for any dissolution profile of any new submitted experimental batch (assuming the experimental conditions have been maintained as those of the training set). The use of ANNs is nevertheless limited, as they cannot provide any information at all about the underlying mechanisms of drug dissolution and diffusion. It was in this context that Reis *et al.* [12]

showed the usefulness of the ANN methodology by applying it to real experimental systems, namely the hydrocortisone in a biodegradable matrix and rhodium (II) butyrate complexes in bioceramic matrices. The training set consisted of hydrocortisone experimental data compiled by Fu *et al.* [5] plus artificial data created using the Higuchi equation with variation of the physicochemical parameters of Fu *et al.* [5] within specified bounds. They have shown that submitting a new unknown experimental data set to the neural network the algorithm was able to recover the input parameters of the formulation (drug solubility, initial drug loading and radius and thickness of tablet) for short and long time period releases. They have nevertheless noted that either ANNs or conventional methods, as nonlinear regression analysis, only provide a single possible set of parameters for some experimental release profile as this is essentially a multivariate problem.

Therefore it is desirable from the experimental point of view to have a whole spectrum (not necessarily complete) of physicochemical parameter values for some matrix that once combined reproduce its fiducial drug release fractions at pre-specified intervals of time. With this background data new unforeseen experimental paths may be explored in order to get new matrix compositions and geometries that may be economically more viable yet

In the following sections, we show how the above multivalued parameter problem can be casted into a numerical optimization problem generally known as multimodal function minimization. We subsequently describe the methodology used in this work, which is based on the coupling of a genetic algorithm with fuzzy logic. We use the Higuchi semi-empirical model (Section II A) in our benchmarks due to its analytical simplicity and widespread use. Nevertheless the proposed algorithm can be easily applied to any other more sophisticated drug release model, but with a possible higher cost in computational resources.

II. METHODOLOGY

A. Drug release mathematical formulation

Following our previous work [12] we use the model proposed by Higuchi [7] for our fiducial controlled release profile of HPMC tablets. This theoretical model was originally proposed with the intent of studying the release of drug molecules from creams and ointments, but since then has found widespread use in controlled delivery systems based on HPMC [2, 15].

Higuchi [7] assumed a one-dimensional system (slab model) under pseudo-steady conditions which generally cannot be applied to real controlled released systems. As illustrated in Fig. 1 the model assumes that as time evolves three distinct regions along the cross section of a thin tablet appear. In the pristine region III the drug is assumed to be in solid form, finely divided and in an immobile dispersed state within the matrix with some constant initial concentration C_0 . As the tablet enters in contact with some external medium (region I) an intermediate region II starts to develop, where the drug is completely dissolved and with concentration below the solubility limit C_s . As the dissolution front, x_b , moves with time the dissolved drug diffuses through the boundary $x = 0$ to some external reservoir. The external reservoir is assumed to be very large and well-mixed so that perfect sink conditions are maintained at the surface of the carrier ($C(0, t) = 0$). Given this simplified setting a few additional assumptions underpin the derivation of the Higuchi equation: the dissolution rate is faster than the drug diffusion rate; swelling or erosion of the carrier is negligible (dimensions of tablet are kept fixed); the initial loading is much greater than the drug solubility in the matrix ($R = C_s/C_0 \ll 1$); and finally the concentration profile is linear inside the depletion zone (region II in Fig. 1). This pseudo-steady state is a reasonable approximation as long as there is a relatively large excess of dispersed solute ($R \leq 1$). The moving front, $x_b(t)$, will then be located so that the mass of drug which has dissolved and left region III is equal to the mass diffused across the boundary $x = 0$. Using the Fick's second law of diffusion at boundary $x = 0$ [3] one can easily derive an expression for x_b :

$$x_b(t) = \left[\frac{2DRt}{1 - R/2} \right]^{\frac{1}{2}}. \quad (1)$$

From Eq. 1 one can derive the cumulative mass fraction of suspended drug, $Q(t)$, that has been released to the external medium:

$$Q(t) = \left[\frac{2RD}{L^2} \left(1 - \frac{R}{2} \right) \right]^{\frac{1}{2}} t^{1/2} \quad (2)$$

where $Q(t) = M_D(t)/M_{\text{tot}}$, with M_D and M_{tot} being respectively the diffused and total drug masses, D is the effective diffusivity of the drug molecules in the matrix substance, assumed to be constant, and L is the total thickness of the topical formulation.

Equation (2) remains valid as long as R is significantly small. Once the parameter R approaches unity, when most of the drug has dissolved, the pseudo-steady state is no longer

valid and subsequent drug diffusion is governed by some unsteady-state diffusion solution (see [1]). The exact solution for the above simplified model with drug in suspension for all concentration ratios $R < 1$ was found by Paul and McSpadden [11], who do not assumed a linear drug concentration within the dissolved zone. Although more complicated than the Higuchi solution (Eq. 2), their exact solution confirms the power-law behaviour with time as long as some drug remains in the solid phase. Bunge [1] made a thoroughly comparison between predictions of the Higuchi approximation and the exact solution by varying the parameter R . She found that the Higuchi approximation underpredicts the cumulative mass released by a few ten percent when R approaches unity. A direct consequence of this is that the relative error of the constant of diffusion, D , if estimated from experimental data of the cumulative mass released, may reach about 30%. The Higuchi approximation also overpredicts the time required for complete dissolution of the drug. In order to minimize these differences, Bunge [1] proposed a simple modification of Eq. 2:

$$Q(t) = \left[\frac{2RD}{L^2} \left(1 - \frac{R(\pi - 2)}{\pi} \right) \right]^{\frac{1}{2}} t^{1/2} \quad (3)$$

Despite all the above restrictions, the Higuchi approximation still provides a reasonable description of the mass released from suspended drugs with $0 < R < 1$ (see Fig.5 from Bunge [1]) and thus we will use Eq. 2 in the forthcoming sections. We should refer in passing that the proportionality between the fractional amount of drug released and the square-root of time can be also derived from different physical grounds, namely from the diffusion of the drug not initially present in solid form, that is with $C_0 < C_s$, for thin films under perfect sink conditions and constant diffusivity [3].

We remind the reader that if one assumes a more complicated device geometry or a more comprehensive mechanistic theory, more complex non-analytical descriptions will be obtained for the drug release rates (for the slab geometry with more elaborated release kinetics see for example [4, 9] and references therein; for cylindrical geometries see the comprehensive reviews in [14, 15, 16]). However if one intends to have a first hand knowledge of a new topical formulation, then the Higuchi power-law approximation will suffice and will have the extra advantage of low computational cost.

B. Fuzzy-controlled genetic algorithmic approach

According to Higuchi's power-law (Eq. 2) the constant of proportionality incorporates all the structural and geometric characteristics of the carrier device and so a multitude of physically acceptable combinations of the parameters C_0 , C_s , D and L can give equivalent mass release profiles. We propose in this section a methodology based on genetic algorithm fundamental concepts for finding all relevant sets of parameters $\vec{\chi} = \{C_0, C_s, D, L\}$ that give the same mass release profile Q as some chosen reference profile Q_{ref} . In the present work we adopt an artificial reference profile, Q_{ref} , the same as that introduced by [12] to validate their neural network model of controlled drug release (see Table I). Let us then define the following functional:

$$\mathcal{F}(Q(\vec{\chi})) = \log \left| \frac{Q(\vec{\chi}; t)}{Q(\vec{\chi}_{\text{ref}}; t)} - 1 \right|, \quad (4)$$

where the function Q is given by Eq. 2 and $\vec{\chi}_{\text{ref}}$ is the vector of parameters for our reference profile. Recall that \mathcal{F} is independent of the time variable, t , because Q is a power-law, but if Q has a different functional form, one or more instants of time (e.g. the dissolution time) needs to be added to the parameter space $\vec{\chi}$. From now on we will drop the variables from the definition of Q to avoid cluttering of the equations. One can easily see that the function \mathcal{F} diverges whenever the trial function Q tends to Q_{ref} . Moreover as expected, there is more than one solution Q for which \mathcal{F} diverges, as can be seen by inspection of Figures (2) and (3). There we plot the projections of the 4-dimensional landscape of the function \mathcal{F} on all planes defined by the pairing of the variables C_0 , C_s , D and L . Distinctive features are revealed in those figures, namely an aligned set of disjoint regions with negative elliptical contours present in all projections of \mathcal{F} . As these regions are zoomed up (Fig. 3) the elliptical contours merge to form long ridges that in turn reveal another set of elliptical contoured regions of decreasing value of \mathcal{F} in a self-similar fashion. Given this, one easily realizes that the set of minima simply correspond to the set of mass release functions, $Q = K(\vec{\chi})t^{1/2}$, for which $|K - K_{\text{ref}}| < \epsilon$ with ϵ being very small. That is, one can cast the combinatorial problem of finding all possible combinations among the parameters $\{C_0, C_s, D, L\}$, that give almost the same value of K_{ref} , to the optimization task of locating all minima in the 4-dimensional hyper-surface of \mathcal{F} as defined in Eq. 4. To solve this optimization problem we make use of a special adaptive genetic algorithm technique (hereinafter aGA) whose control parameters

evolve dynamically according to fuzzy logic rules as the search procedure progresses.

Standard genetic algorithms are known to be a particularly good approach for optimization problems that require finding either a unique global solution or more than one solution like the work discussed in here (see for example [6, 10]).

Unlike local traditional optimizers, like the first-order (steepest descent, conjugate gradient) and second-order (quasi-Newton) methods, GAs are stochastic search methods not strongly influenced by the initial trial solution. This is because the genetic algorithm paradigm consists in evolving a group of candidate solutions (population) throughout a number of steps, where at each new step (generation) a new group of solutions is created from the previous one by a set of transformations. These transformations, inspired by the laws of natural selection, comprise the basic operations of recombination of the information encoded in some probabilistically selected pairs of solutions among the population accompanied by some random alteration of the encoding in their offspring. The fittest members of the population of solutions according to some figure of merit, the fitness function, will pass onto the next generations preserving most of their optimal information [6]. All this enables the GA method to explore new points in the search space and proves quite effective in locating the global minimum of some complicated functions which is masked by a plethora of local minima and could not possibly be found by the more traditional search procedures (unless of course some finely tuned initial trial solution is provided in the neighborhood of the global minimum, but that is completely unknown *a priori*). The choice of GA parameters, such as the selection method for crossover and mutation operations and their associated frequency of occurrence, determines the balance of exploration of search space and the exploitation of information contained in the population. It is the adequacy of this balance that leads to the successful application of a GA in unimodal problems, but reveals itself somewhat insufficient for multimodal problems such as one formulated here. One of the possible causes is that the GA parameters (selection pressure of tournament selection for crossover, probability of occurrence of random mutation, population number) are pre-fixed and kept constant throughout the search run. While at the early stages of the search the GA exploration is the dominant mode, quickly exploitation of only a few good solutions will take over and we might end up by finding only a few "target" regions of the solution space. One improvement could be rerunning the GA with different sets of control parameters and initial populations, but that might reveal itself costly in computational resources. Instead

we try to ameliorate this situation by introducing new genetic operators and by letting the GA control parameters evolve adaptively along the GA run according to fuzzy logic rules (for an introduction to fuzzy logic see the book by Jang and Sun [8]). Three new genetic operators are introduced: the predator operator, a new niche operator that we call the habitat operator and finally the immigration operator. They are all designed in order to preserve "speciation", that is, to locate new distinct clusters (species) of solutions and to preserve as best as possible the neighborhoods around local minima already found by the algorithm.

We proceed to describe the main features of the new proposed adaptive genetic algorithm (aGA). The search run is started with a population of 100 trial profiles each of which represented by a 4-dimensional vector $\vec{\chi}$. As in the standard GA, the real components of the vectors are encoded into binary strings and these are concatenated to form a long string to represent the vector $\vec{\chi}$, called in the GA jargon by chromosome. The search space of each of the vector components of $\vec{\chi}$ is bounded by the pairs of limits listed in Table I. We require that multiple solutions $\vec{\chi}$ found by the aGA can be distinguished experimentally so we must restrict the precisions (number of digits after the decimal point) of their components accordingly. Given the ranges listed in Table I and representing each decade with ~ 3 bits, we encode each of the components C_0 , C_s , D , L with 10, 10, 14 and 6 bits respectively. This means that a total of 40 bits are necessary to represent the whole vector $\vec{\chi}$. The ranges in Table I define an envelop around the reference Higuchi profile $Q(t; \vec{\chi}_{\text{ref}})$ and we always start the aGA with a population of random profiles but constrained to this region.

As the aGA is designed to give multiple profile solutions one needs to find only the most representative ones and eliminate very similar profiles. We do that by grouping several solutions into sets of clusters (classes), each of which contains profiles that have very similar parameters according to the classification system that will be described later.

Operadores Genéticos

O processo de evolução natural submete os seres vivos ao procedimento de seleção natural que pode ocorrer através da eliminação dos indivíduos menos adaptados por meio de predadores ou morte natural (doenças e velhice) ou ao favorecimento dos indivíduos mais adaptados através principalmente do processo de reprodução que pode ser intensificados pela longevidade do indivíduo. Portanto o processo de reprodução é favorecido em populações com elevado índice de adaptação enquanto que o processo de mutação torna-se mais favorável em populações com baixo índice de adaptação. A partir deste raciocínio inicial o algoritmo genético desenvolvido apresenta uma associação com a teoria de controladores fuzzy que deverão determinar qual a taxa de execução de cada operador genético em cada geração. Na estrutura do GA foram adicionados também os seguintes operadores: predador, imigração e habitat. Cada controlador fuzzy determina a probabilidade de execução de cada operador genético sobre um ou mais indivíduos. As funções de pertinência são calibradas a cada geração, para os operadores: predador, crossover, mutação e imigração as funções de pertinência dependem da distribuição normal dos valores da função fitness, Os controladores utilizam a média da função fitness na população (M) e o desvio padrão da função fitness (D_m). A probabilidade dos operadores: predador, crossover e mutação dependem também do valor de fitness de cada indivíduo que será submetido ao procedimento realizado pelo operador genético. O operador habitat apresenta uma dependência com a distância euclidiana entre os indivíduos analisados. Enquanto o operador genético imigração depende da atividade dos operadores predador e habitat através da quantidade de indivíduos eliminados da população (N). É importante lembrar que o valor da função fitness corresponde ao logaritmo do erro absoluto e portanto deve ser minimizado, ou seja, quanto menor o erro mais adaptado será o indivíduo.

O operador predador elimina indivíduos da população de acordo com a probabilidade definida como uma função sigmoideal aberta para a direita, portanto quanto maior o valor de fitness maior a probabilidade de o indivíduo ser eliminado da população. A maior probabilidade de eliminação aparece para indivíduos que tem o valor Fitness superior $M+D_m$.

O operador habitat garante que a população não irá convergir para uma única solução. Sempre que um indivíduo estiver muito próximo de outro, ocorrerá um aumento na probabilidade de execução de um torneio (P_{hab}) entre os indivíduos próximos. Neste torneio a probabilidade de eliminação (eq. 5) é utilizada para definir qual indivíduo está mais adaptado e consequentemente terá menor probabilidade de ser retirado da população. O operador habitat outorga a cada indivíduo a responsabilidade de otimizar uma região do espaço de busca que apresenta formato esférico, fazendo com que dentro da faixa de erro não existam dois ou mais indivíduos para uma mesma região do espaço. A função de pertinência do operador habitat depende do raio de ativação do operador habitat (R_m), que corresponde a distância euclidiana mínima para evitar o torneio. O valor do raio de ação depende da soma da variação mínima entre os parâmetros, desta forma o R_m depende diretamente da precisão de cada parâmetro e consequentemente da quantidade de bits utilizada para representar os indivíduos. Na determinação dos parâmetros C_0 , C_s , D e h o valor de R_m deve ser igual a 0.13.

Table 1 Funções de pertinência para o controle dos operadores genéticos.

Operador	Função de Pertinência	Parâmetros
Predador Eq 5	$P(F_i, M, D_m)_p^i = \frac{1}{1 + e^{-\frac{1}{M+D_m}(F_i-M+D_m)}}$	
Habitat Eq 6	$P(R_{ij})_{hab}^{ij} = \frac{1}{1 + e^{-(R_{ij}-R_m)}}$	$R_m=0.13$
Imigração Eq 7	$N(N_{(p+hab)}, M, D_m)_{imi} = \frac{N_{(p+hab)}}{2 \left(1 + e^{-\frac{1}{M+D_m}(M-A_i)} \right)}$	$A_i=1.3$
Crossover Eq 8	$P(F_i, F_j, M, D_m)_{cross}^{ij} = \frac{1}{1 + e^{-\frac{1}{M+D_m}(F_i-M-D_m)}} \times \frac{1}{1 + e^{-\frac{1}{M+D_m}(F_j-M-D_m)}}$	
Mutação Eq 9	$P(F_i, M, D_m)_{mut}^i = p_m \frac{1}{1 + e^{-\frac{1}{M+D_m}(F_i-M+D_m)}}$	$P_m=0.03$

O operador imigração cria novos indivíduos aleatórios, diminuindo a degenerescência da população e evitando a convergência prematura do algoritmo genético. A quantidade máxima de indivíduos criados aleatoriamente (N_i) é definida pela eq. 7 (sigmóide aberta para a direita) e é limitada pela metade dos indivíduos eliminados pelos operadores predador e habitat. O controle fuzzy realizado sobre o operador de imigração, cria novas regiões de otimização enquanto a população ainda se encontra dispersa, ou seja, apresenta um valor de fitness elevado. No momento que a população esta se aproximando do limite de convergência, o operador imigração tem sua atividade praticamente anulada. O parâmetro A_i representa o valor limite para a função fitness onde o operador começa a perder expressividade, pois a população encontra-se bem adaptada, o valor 1.3 foi determinado empiricamente variando o parâmetro A_i entre 0 e 2 que corresponde ao intervalo fitness inicial do GA.

A probabilidade para a execução do operador crossover é definida como a t-norma probabilística de dois indivíduos selecionados aleatoriamente. Este processo de ativação do operador crossover assemelha-se a estratégia de seleção denominada torneio, em que o indivíduo mais adaptado eleva a probabilidade de transferência de suas informações para os novos indivíduos da população. Sendo a t-norma probabilística o produto de duas funções de pertinência (eq. 8) a função de probabilidade apresenta-se mais restritiva, como pode ser observado na figura XX com o deslocamento da curva para a esquerda, ou seja para a região de maior adaptação.

O operador mutação, assim como o operador imigrante apresenta a capacidade de reduzir a degenerescência da população e criar novas localidades de otimização evitando os possíveis mínimos locais. A probabilidade de mutação apresenta uma penalidade intrínseca (P_m) que limita o valor de probabilidade de ocorrência do operador mutação. O valor P_m foi determinado empiricamente entre 0 e 1, se $P_m \sim 1$ o operador mutação é executado excessivamente inserindo assim um comportamento aleatório na população que ira demorar demasiadamente para convergir.

A cada geração os indivíduos são agrupados em classes definidas de acordo com a distância euclidiana dos vetores unitários dos membros da população. Dentro de uma classe a distância máxima entre dois indivíduos não pode ser superior a 1% do espaço de busca, este valor limite influencia na quantidade e na precisão das soluções finais. Cada solução é definida como sendo o centro de massa de cada classe. No instante em que as classes são formadas os indivíduos que apresentam um valor de fitness inferior a $M-D_m$ são selecionados como soluções especiais, pois em media apresentam um erro de ajuste 10 vezes menor que as soluções normais. A convergência do GA ocorrerá em duas situações distintas:

- i) O GA terá convergido se somente se operadores predador e habitat não forem mais capazes de eliminar indivíduos devido à convergência de toda a população para um único valor de erro de ajuste.
- ii) O GA será finalizado se somente se $\log(\text{Erro}_m) \leq \log(\text{Erro}_{\text{limite}})$ e sendo $\log(\text{Erro}_{\text{limite}}) = -6$. O valor de $\text{Erro}_{\text{limite}}$ foi escolhido para garantir que as curvas de liberação controlada determinadas pelo GA sejam indistinguíveis experimentalmente da curva de referencia (Tabela 1)

Resultados e discussões

O modelo desenvolvido por Higuchi (eq. 2) foi utilizado neste trabalho como base para a definição do espaço de busca e geração da curva problema para o algoritmo genético a partir dos valores de referência. A validade do modelo teórico é descrita no trabalho de Fu e colaboradores, que demonstram a partir de dados experimentais que a eq. 2 pode ser utilizada para descrever a fração liberada de hidrocortisona. Como descrito anteriormente o modelo apresenta uma constante de proporcionalidade que relaciona a concentração inicial da hidrocortisona (C_0), a concentração de saturação (C_s), o coeficiente de difusão (D) e a altura do dispositivo (h).

A limitação do espaço de busca do algoritmo genético foi realizada a partir dos parâmetros (C_0 , C_s , D , h) utilizados por Reis e colaboradores, que utilizaram as curvas de liberação controlada de hidrocortisona para o treinamento de uma rede neuronal que apresentava como saída o conjunto de parâmetros (C_0 , C_s , D , h) que gera cada curva. O espaço de busca do algoritmo genético será limitado por duas curvas de liberação, a primeira apresenta os valores máximos do espaço de busca e corresponde experimentalmente a matriz de polycaprolactone que apresenta uma liberação de 60% da hidrocortisona em 100 dias. A segunda curva apresenta a menor fração de hidrocortisona liberada (3% em 100 dias) e é gerada pelos parâmetros com valores inferiores de C_0 , C_s , D e h . A faixa de variação de cada parâmetro é bem diferenciada, como pode ser observado na tabela 1, o coeficiente de difusão apresenta uma variação de 100 vezes dentro do intervalo que vai de $0,042 \times 10^{-5}$ até $4.85 \times 10^{-5} \text{ cm}^2 \text{ dia}^{-1}$. Para o modelo de Higuchi (eq. 2) apenas a altura do comprimido será otimizada, o raio do comprimido é de 1.5 cm e a altura pode varia entre 0.164 e 0.170cm. O valor da concentração inicial C_0 pode variar entre 33.3 e 133.1 $\text{mg} \cdot \text{cm}^{-3}$ que corresponde a aproximadamente 4 vezes enquanto que C_s pode ser determinado dentro da faixa de 2.7 e 40.0 $\text{mg} \cdot \text{cm}^{-3}$ variando em até 15 vezes em relação o limite inferior. Esta diferença de ordem de

variação reflete na quantidade de bits utilizada para representar cada parâmetro. O algoritmo genético foi desenvolvido para encontrar múltiplas soluções para uma curva de liberação controlada de fármacos, desta forma a precisão do conjunto de dados é determinante para que o sistema não encontre soluções que experimentalmente sejam indistinguíveis. Utilizando a relação de 3.3 bits para cada ordem de grandeza os valores do coeficiente de difusão foram obtidos com uma representação de 14 bits, para os parâmetros C_0 , C_s e h foram utilizados respectivamente 10, 10 e 6 bits, ou seja, o conjunto de parâmetros utiliza 40 bits, que poderão representar soluções com a quantidade de algarismos significativos compatível com a precisão experimental.

Os parâmetros referentes ao algoritmo genético foram determinados através de testes considerando principalmente a razão entre a quantidade de soluções encontradas pela quantidade de gerações até a convergência. O tamanho da população é de 100 indivíduos, as taxas de crossover, mutação, imigração e eliminação são controladas a cada geração pelos controladores fuzzy. O controle dos operadores predador e crossover dependem apenas da média e do desvio padrão dos valores da função fitness a cada geração. A calibração dos outros operadores depende de constantes que foram determinadas empiricamente através da execução do operador a ser calibrado juntamente com os operadores predador e crossover.

O valor médio da função fitness apresenta uma elevada quantidade de oscilações que são provocadas pelas ativações e desativações dos operadores que minimizam o erro (crossover, predador) contra os operadores de diminuem a degenerescência da população (mutação, imigração e habitat). Para cada população de 100 indivíduos o GA encontra entre 12 e 24 soluções diferentes para uma quantidade de gerações que pode variar de 7000 a 9000

A curva de referencia foi gerada a partir de parâmetros (C_0 , C_s , D e h) que fornecem uma fração liberada de hidrocortisona de 30%. Esta curva pode ser gerada a partir dos seguintes parâmetros definidos como ideais $D_{(ideal)} = 1.35 \text{ cm}^2 \text{ dia}^{-1}$; $C_{0 \text{ (ideal)}} = 70.0 \text{ mg cm}^{-3}$; $C_{s(ideal)} = 16.2 \text{ mg cm}^{-3}$ e $h_{ideal} = 0.167 \text{ cm}$.

Para os intervalos de busca definidos na tabela 1 o algoritmo genético encontrou 568 soluções diferentes para os parâmetros (C_0 , C_s , D , e h), sendo que 30 soluções estão na tabela 3 e todas apresentam um erro de ajuste da função de fração liberada de hidrocortisona e aproximadamente $10^{-2}\%$. Dentre as diversas soluções encontradas destaca-se a solução 1 que corresponde aos parâmetros de referência, atestando assim a capacidade da metodologia em determinar a solução global em problemas com múltiplas soluções. Como o coeficiente de difusão pode variar em até 100 vezes, pequenas alterações no valor do coeficiente de difusão podem gerar soluções completamente distintas como ocorre com as soluções 10, 11 e 12 em que o valor de D é $0.888 \times 10^{-5} \text{ cm}^2 \text{ dia}^{-1}$ para as soluções 10 e 12 enquanto na solução 11, o valor de D é de $0.876 \times 10^{-5} \text{ cm}^2 \text{ dia}^{-1}$, com uma variação de 1.3%, entretanto, a mesma convergência de valores não é observada para os valores de C_0 e C_s que variaram aproximadamente 75%. Outras relações semelhantes podem ser observadas como por exemplo, nas soluções 22 e 24, ou nas soluções 17 e 18. Aproximadamente dois terços de todas as soluções apresentam coeficiente de difusão inferior ao valor de referência ($1.35 \times 10^{-5} \text{ cm}^2 \text{ dia}^{-1}$),

esta distribuição tendenciosa é esperada devido a fração total de hidrocortisona liberada ser de apenas 30%. De acordo com Fu e colaboradores a o coeficiente de difusão da hidrocortisona na matriz de PVA terpolymer é de $0.950 \times 10^{-5} \text{ cm}^2 \text{ dia}^{-1}$, que corresponde à solução 2 e aproxima-se das soluções 17 e 18 este resultado demonstra que a matriz polimérica pode ser alterada sem modificar a fração de droga liberada a partir de modificações na outras propriedades (C_0 , C_s e h). As soluções 3, 4 e 5 apresentam respectivamente os parâmetros de referência (C_0 , C_s e h) cada um em uma solução, demonstrando que é possível construir sistemas de liberação controlada de fármacos equivalentes utilizando matrizes completamente diferentes. A partir das diversas soluções encontradas para o conjunto de parâmetros (C_0 , C_s , D e h) a construção de dispositivos de administração da hidrocortisona (Comprimidos) pode ser orientada em função de questões econômicas, mas mantendo a fração de fármaco liberada, ou por questões clínicas, como por exemplo, aumento ou diminuição da dose administrada a um paciente, mas mantendo a taxa de liberação controlada.

Table 2 Representative drug release profiles found by the GA that are equivalent to our reference profile Q_{ref}

	D ($\times 10^{-5} \text{ cm}^2 \text{ dia}^{-1}$)	A ($16.2 \text{ mg} \cdot \text{cm}^{-3}$)	C_s ($16.2 \text{ mg} \cdot \text{cm}^{-3}$)	H (cm)
1	1.350	70.1	16.2	0.1670
2	0.950	65.5	23.6	0.1685
3	0.992	70.1	23.0	0.1660
4	1.790	94.2	16.2	0.1685
5	1.530	37.4	7.45	0.1670
6	4.016	42.8	3.0	0.1650
7	1.356	54.7	13.1	0.1700
8	1.331	97.6	23.6	0.1691
9	1.026	119.2	36.6	0.1641
10	0.888	73.1	29.4	0.1698
11	0.876	46.5	18.4	0.1675
12	0.888	80.8	32.6	0.1698
13	2.725	46.6	4.9	0.1654
14	2.419	130.4	15.9	0.1672
15	0.820	50.1	22.2	0.1690
16	2.739	46.2	4.9	0.1666
17	0.953	108.5	38.0	0.1667
18	0.940	68.7	23.8	0.1649
19	0.722	33.8	17.7	0.1680
20	0.876	46.5	18.4	0.1675
21	1.173	121	31.7	0.1643
22	0.798	87.4	39.8	0.1684
23	3.055	73.0	6.7	0.1643
24	0.796	70.7	32.7	0.1691
25	0.616	57.1	36.6	0.1646
26	0.812	77.1	33.2	0.1664
27	0.992	70.0	23.0	0.1659
28	1.125	126.0	36.7	0.1682
29	4.676	120.4	7.3	0.1668
30	1.714	108.9	20.0	0.1699

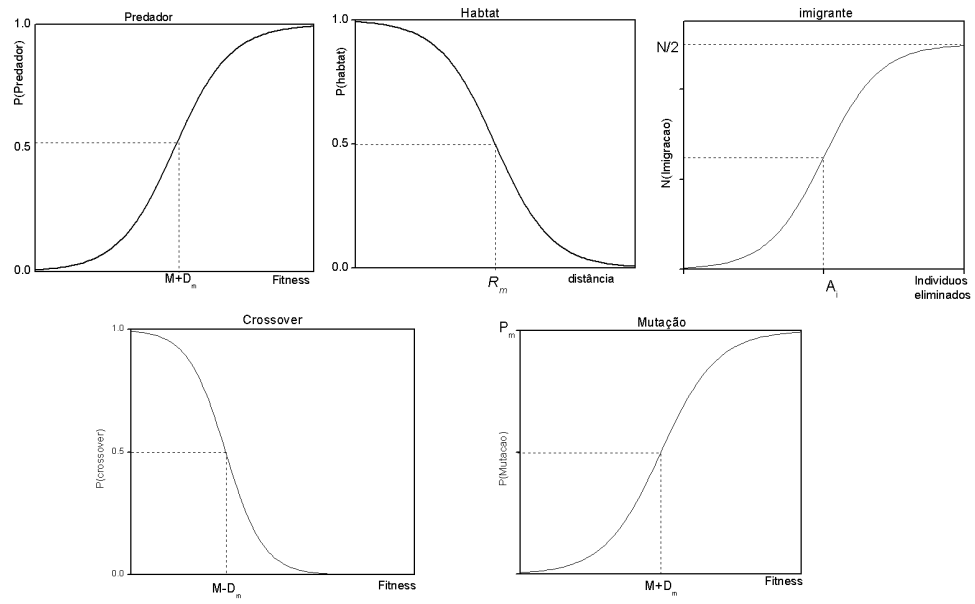


Figura 4 Perfil das funções de pertinência para controle dos operadores genéticos.

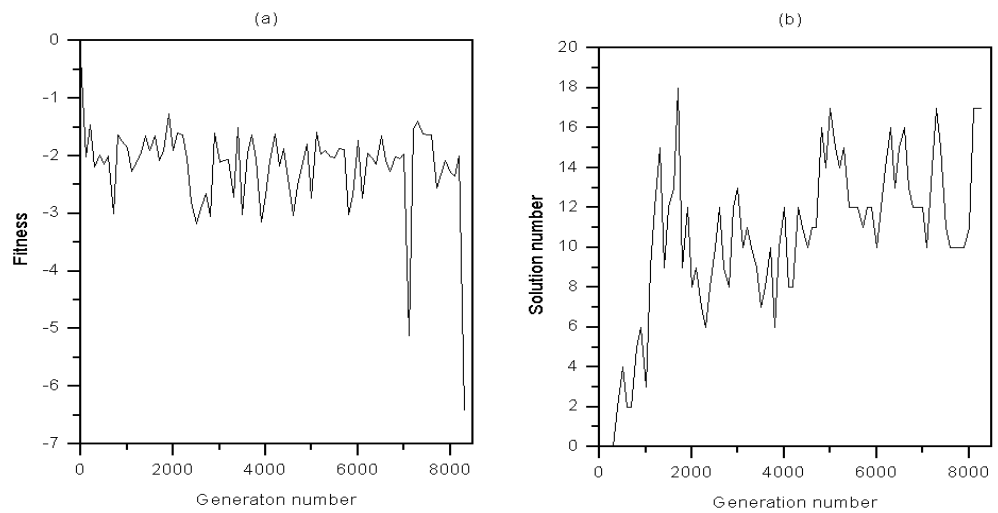


Figura 5 (a) Evolução do valor médio da função fitness (eq. 4) em função do número de gerações. (b) Quantidade de possíveis soluções em cada geração do GA..

IV. CONCLUDING REMARKS

We have argued in this work the technological importance of being able to estimate sets of possible combinations of physicochemical properties of a drug-matrix system that can achieve the same desired drug controlled release profile. This ability allows a rapid and efficient assessment of the economical viability of the different paths of tablet manufacturing that might be proposed according to the therapeutic goal of the drug, the physiological medium where the drug is supposed to be most effective or the timing of some fixed drug fraction. Evidently not all parameter combinations might be experimentally possible, but that provides precisely the argument in favour of being able to generate large batches of parameters at once so that one can quickly inspect and select the most feasible combinations.

The adaptive genetic algorithm presented in this article proved to be an efficient tool in realizing the above goals. Despite the test case being mathematically a simple one, namely the Higuchi power-law where all physicochemical parameters are combined into just a single factor, it reveals itself difficult in practice to find systematically all desired combinations without the aid of some intelligent system. One must also remind the reader that this genetic algorithm is a general search tool which does not require the controlled release model to be expressed analytically. All that the GA requires from a release model is the evaluation of the fitness function, either by direct evaluation of some analytical expression or by the numerical resolution of a set of coupled differential equations (e.g. [14, 16]) at the expense of higher computational demands and slower convergence. In any case one might also need to further tailor the genetic operators since the dimensionality of the search space can increase as well as the complexity of its topology. Finally, if one is not only interested

in obtaining sets of parameters that originate release profiles infinitely similar to the desire one, but also profiles which lie within some envelop all we need is to relax the convergence criterion.

Acknowledgments

- ¹ Bunge, A. L., 1998, J Control Release **52**(1-2), 141.
- ² Costa, P., and J. M. Sousa Lobo, 2001, European Journal of Pharmaceutical Sciences **13**(2), 123, URL <http://www.sciencedirect.com/science/article/B6T25-43JXG27-2/2/5e4aec3da6423036b39fb65cf092c2e8>.
- ³ Crank, J., 1975, *The Mathematics of Diffusion*, SBN: 0198533446 (Clarendon Press).
- ⁴ Frenning, G., 2003, J Control Release **92**(3), 331.
- ⁵ Fu, J. C., C. Hagemer, and D. L. Moyer, 1976, J Biomed Mater Res **10**(5), 743, URL <http://dx.doi.org/10.1002/jbm.820100507>.
- ⁶ Goldberg, D., 1989, *Genetic Algorithms in Search, Optimization, and Machine Learning* (Addison-Wesley Professional), URL <http://www.amazon.ca/exec/obidos/redirect?tag=citeulike09-20&path=ASIN/0201157675>.
- ⁷ Higuchi, T., 1961, J Pharm Sci **50**, 874.
- ⁸ Jang, J.-S. R., and C.-T. Sun, 1997, *Neuro-fuzzy and soft computing: a computational approach to learning and machine intelligence* (Prentice-Hall, Inc.).
- ⁹ Kalia, Y. N., and R. H. Guy, 2001, Adv Drug Deliv Rev **48**(2-3), 159.
- ¹⁰ Kao, Y.-T., and E. Zahara, 2008, Applied Soft Computing **8**(2), 849, URL <http://www.sciencedirect.com/science/article/B6W86-4P4NPDM-2/2/fdda99066f98e78332467adbb72ab177>.
- ¹¹ Paul, D. R., and S. K. McSpadden, 1976, Journal of Membrane Science **1**, 33, URL <http://www.sciencedirect.com/science/article/B6TGK-43N87VJ-41/1/ac77c36b66a2b07fc9c3ab983e6a06df>.
- ¹² Reis, M. A., R. D. Sinisterra, and J. C. Belchior, 2004, Journal of Pharmaceutical Sciences **93**(2), 418, URL <http://dx.doi.org/10.1002/jps.10569>.

- ¹³ Siepmann, J., and A. Gpferich, 2001, Adv Drug Deliv Rev **48**(2-3), 229.
- ¹⁴ Siepmann, J., and N. A. Peppas, 2000, Pharm Res **17**(10), 1290.
- ¹⁵ Siepmann, J., and N. A. Peppas, 2001, Adv Drug Deliv Rev **48**(2-3), 139.
- ¹⁶ Siepmann, J., A. Streubel, and N. A. Peppas, 2002, Pharm Res **19**(3), 306.
- ¹⁷ Sun, Y., Y. Peng, Y. Chen, and A. J. Shukla, 2003, Adv Drug Deliv Rev **55**(9), 1201.

List of Figures

- 1 Diagram showing the drug concentration profile at time t in some planar thin matrix of half-thickness $L/2$ (thick line). Diffusion proceeds along the horizontal axis from region II , where the drug is completely dissolved, to an external sink (region III). Meanwhile the boundary between regions 1 and 2, $x_b(t)$, moves in the positive x direction as the suspended drug in region 1 dissolves with time. 15
- 2 Filled contour plots representing the projections of the four-dimensional function \mathcal{F} (Eq. 4) onto the planes (a) $D-C_s$, (b) $D-C_0$, (c) $D-L$, (d) C_s-C , (e) C_s-L and (f) $C-L$. Dashed lines refer to contours with negative values. One can see a distinctive stratigraphic ridge across all projection planes onto which the function \mathcal{F} diverges to minus infinity. 16
- 3 These plots are the zoomed up square regions in black of the previous Figure. One can see that the ridges consist of several local minima. Their number and depth will increase as the image is more finely resolved. 17

List of Tables

- I Parameters defining the reference profile and its envelop delimited by the upper and lower curves. These simulation parameters were used for the training of the neural network model proposed by [\[12\]](#) and are also adopted as a benchmark of the present algorithm. Note that the size of the envelop actually encompasses the four different matrices analyzed by Fu *et al.* [\[5\]](#) for the experimental release of hydrocortisone ($\sim 3\%$ – $\sim 60\%$ release after 100 days). 18
- II Representative drug release profiles found by the aGA that are equivalent to our reference profile Q_{ref} . The last column shows the deviation 19

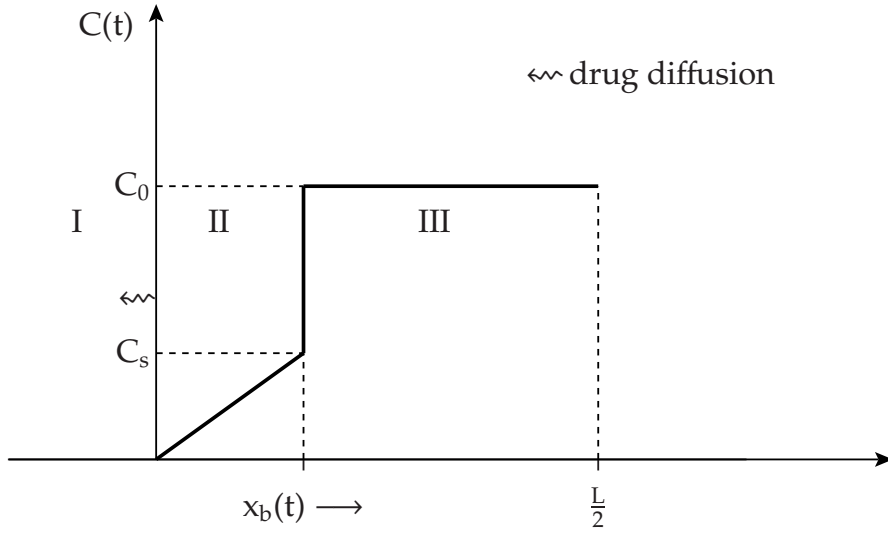


FIG. 1: Diagram showing the drug concentration profile at time t in some planar thin matrix of half-thickness $L/2$ (thick line). Diffusion proceeds along the horizontal axis from region II , where the drug is completely dissolved, to an external sink (region III). Meanwhile the boundary between regions 1 and 2, $x_b(t)$, moves in the positive x direction as the suspended drug in region 1 dissolves with time.

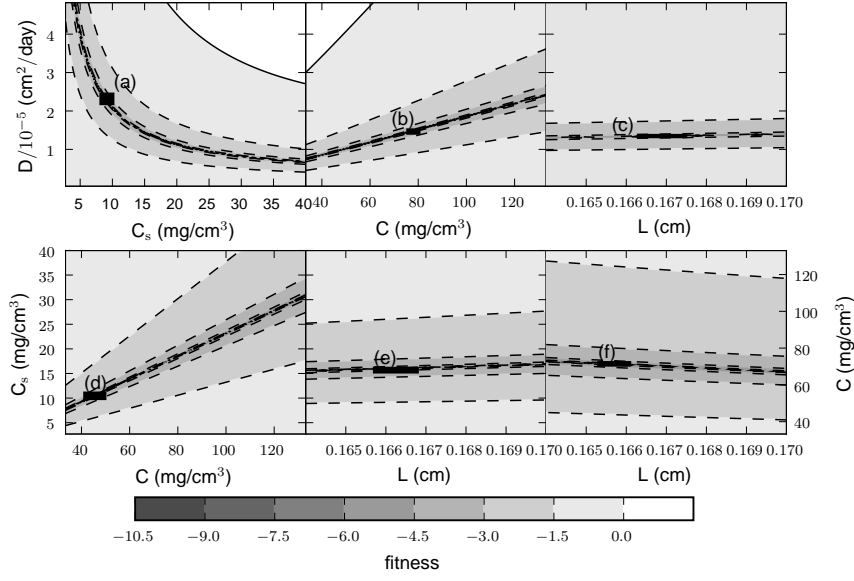


FIG. 2: Filled contour plots representing the projections of the four-dimensional function \mathcal{F} (Eq. 4) onto the planes (a) D - C_s , (b) D - C_0 , (c) D - L , (d) C_s - C , (e) C_s - L and (f) C - L . Dashed lines refer to contours with negative values. One can see a distinctive stratigraphic ridge across all projection planes onto which the function \mathcal{F} diverges to minus infinity.

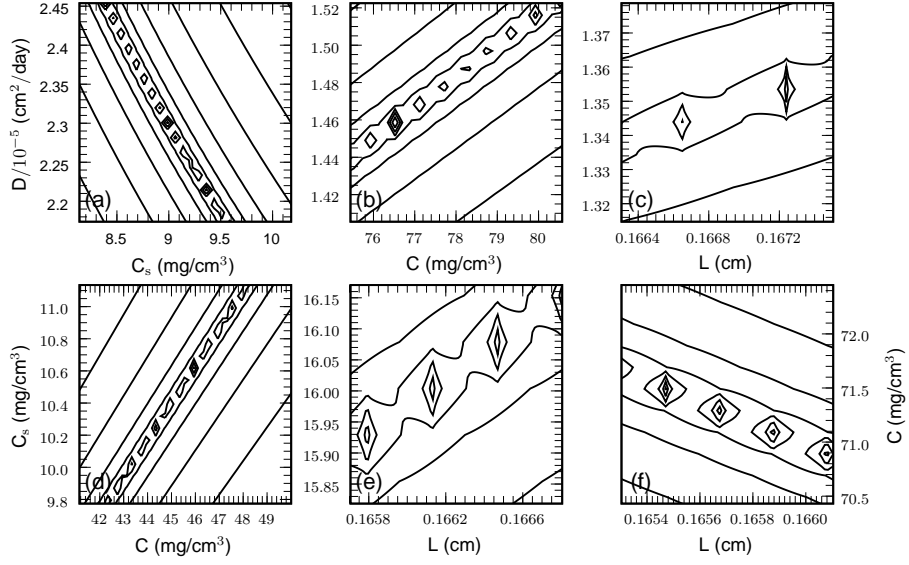


FIG. 3: These plots are the zoomed up square regions in black of the previous Figure. One can see that the ridges consist of several local minima. Their number and depth will increase as the image is more finely resolved.

TABLE I: Parameters defining the reference profile and its envelop delimited by the upper and lower curves. These simulation parameters were used for the training of the neural network model proposed by [12] and are also adopted as a benchmark of the present algorithm. Note that the size of the envelop actually encompasses the four different matrices analyzed by Fu *et al.* [5] for the experimental release of hydrocortisone ($\sim 3\% - \sim 60\%$ release after 100 days).

Parameter	Reference	Lower bound	Upper bound	bits
$C_0/(\text{mg cm}^{-3})$	70.0	33.3	133.1	10
$C_s/(\text{mg cm}^{-3})$	16.2	2.7	40.0	10
$D/(10^{-5} \text{ cm}^2 \text{ day}^{-1})$	1.35	0.042	4.82	14
L/cm	0.167	0.164	0.170	6

TABLE II: Representative drug release profiles found by the aGA that are equivalent to our reference profile Q_{ref} . The last column shows the deviation ...

C_0	C_s	D	L	ϵ
70.0	23.0	0.992	0.1659	2.1e-07
130.4	15.9	2.419	0.1672	6.2e-03
108.5	38.0	0.953	0.1667	6.7e-03
44.9	23.9	0.731	0.1698	1.2e-02
108.9	20.0	1.714	0.1699	1.3e-02
77.1	33.2	0.812	0.1664	1.4e-02
50.1	22.2	0.820	0.1690	1.5e-02
57.1	36.6	0.616	0.1646	1.7e-02
119.2	36.6	1.026	0.1641	1.8e-02
73.0	6.7	3.055	0.1643	2.0e-02
46.5	18.4	0.876	0.1675	2.1e-02
46.5	18.4	0.876	0.1675	2.1e-02
68.7	23.8	0.940	0.1649	2.4e-02
46.2	4.9	2.739	0.1666	2.6e-02
42.8	3.0	4.016	0.1650	3.4e-02
131.5	33.9	1.190	0.1643	3.4e-02
70.7	32.7	0.796	0.1691	4.3e-02
87.4	39.8	0.798	0.1684	4.9e-02
73.1	29.4	0.888	0.1698	5.1e-02
126.0	36.7	1.125	0.1682	5.4e-02
97.6	23.6	1.331	0.1691	6.0e-02
97.6	23.6	1.331	0.1691	6.0e-02
78.8	39.7	0.713	0.1646	6.2e-02
70.1	16.2	1.350	0.1670	6.2e-02
80.8	32.6	0.888	0.1698	6.7e-02
121.0	31.7	1.173	0.1643	6.8e-02
96.8	9.8	2.787	0.1643	8.5e-02
46.6	4.9	2.725	0.1654	8.5e-02
33.8	17.7	0.722	0.1680	9.0e-02
120.4	7.3	4.676	0.1668	1.3e-01